

CORONAL INTERCONNECTION OF TWO ACTIVE REGIONS OBSERVED IN 3.5–8.0 keV X-RAYS

FRANTIŠEK FÁRNÍK

Astronomical Institute of Czechoslovak Academy of Sciences, Ondřejov, Czechoslovakia

and

H. FRANK VAN BEEK* and ZDENĚK ŠVESTKA

Laboratory for Space Research Utrecht, Beneluxlaan 21, Utrecht, The Netherlands

(Received 5 July, 1985; in final form 14 February, 1986)

Abstract. Using HXIS data, we have studied the further development of the coronal arch extending towards the SE above active region No. 17255 in November 1980. The arch, studied originally by Švestka (1984) disappeared on 10 November (after pronounced revival), but since 9 November HXIS revealed another arch-like structure towards the SW. We have studied the development of this new structure which appeared to be most likely an arch interconnecting AR 17255 with AR 17251, located nearly 30° to the west. This interconnection revived many times during the following days with intensity varying with the activity in both active regions. We have estimated the physical characteristics in this coronal structure and compared them with observations of interconnecting loops made at lower energies by Skylab in 1973. The temperature (maximum values $7.5\text{--}14 \times 10^6$ K) and the density ($1.1\text{--}5.0 \times 10^9$ cm $^{-3}$) are found to be higher than in the Skylab loops (a result that could be expected because the HXIS energy range was harder than that of Skylab) and similar to the values deduced for the earlier arch system extending to the SE. However, much shorter decay times of the brightness variations indicate the presence of conduction in contrast to the SE arch in which conduction was clearly inhibited. This supports the assumption that the SE and SW coronal structures were two different phenomena.

1. Introduction

Švestka (1984) has studied the giant post-flare arch which appeared above AR 17255 on 6 November, 1980 when that region was near the eastern limb. He based his study on HXIS data from the bands 1 and 2 (i.e., energies 3.5–5.5 and 5.5–8.0 keV). From his conclusions we repeat here only three items which are important for our following study: (a) the arch was observed above the limb towards the SE where no other active region existed; (b) the arch revived twice during 25 h after its formation – each time after a two-ribbon flare in the underlying active region; (c) the arch cooled very slowly through radiation (conductive cooling was negligible) and its life-time was about 12 h.

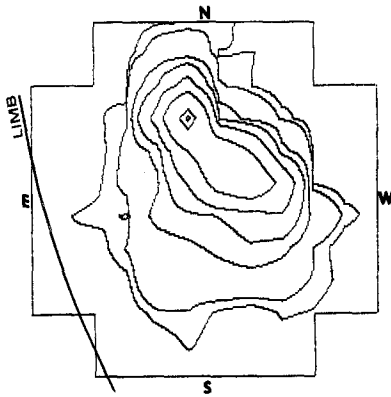
Švestka's study ends after the decay of the second (or third) revival at noon on 7 November when the AR 17255 was still very close to the eastern limb. Originally, the aim of our study was to follow the development of the active region and possible further revivals of the arch after 7 November. But the observations show that after another revival the arch ceased definitely to be visible in X-rays (above 3.5 keV) on 10 November and instead of it we could follow and study a new arch-like structure which appeared towards the SW.

* Presently at Delft Institute of Technology, Landbergstraat 3, 2628 CE Delft, The Netherlands.

2. Observational Data

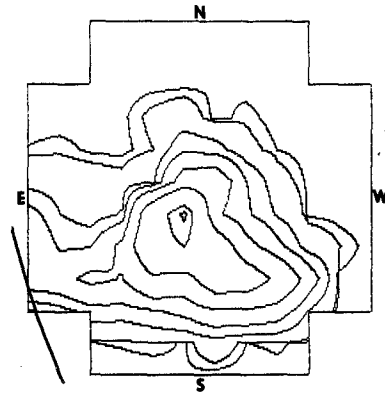
2.1. REVIVED CORONAL STRUCTURES EXTENDING TO THE SE

We began to examine the data from 7 November at noon when the arch after its last known revival ceased to be observable in X-rays. Figure 1(a) shows the AR 17255 later in the afternoon; though the accumulation time was long enough to get the weakest details, no extended coronal structure to the SE appears to be visible. At that time the active region was around 35° from the limb (55° E). The situation remained unchanged



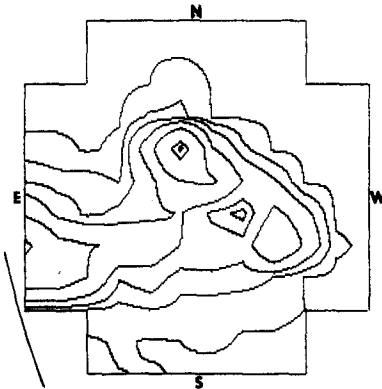
(a) NOV 7, 1980, 19:14 UT

Fig. 1a.



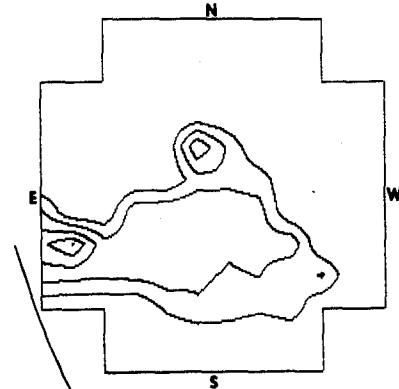
(b) NOV 7, 1980, 23:53 UT

Fig. 1b.



(c) NOV 8, 1980, 01:50 UT

Fig. 1c.



(d) Temperature map

Fig. 1d.

Fig. 1(a-c). 3.5–5.5 keV X-ray images of HXIS coarse field of view centered at AR 17255 on 7–8 November, 1980. The contour levels are 0.5, 1, 5, 10, 20, 40, 80, 95, and 100% of the maximum countrate. (a) 18:49–19:38 UT (accumulation time 1466 s), maximum countrate 0.78 counts s^{-1} per pixel; (b) 23:50–23:56 UT (accumulation time 184 s), maximum countrate 6.7 counts s^{-1} per pixel; (c) 01:33–02:07 UT on 8 November (accumulation time 1006 s), maximum countrate 0.69 counts s^{-1} per pixel. (The 0.5% level is omitted.)

Fig. 1(d). The temperature map derived from the 3.5–5.5 and 5.5–8.0 keV energy bands on 7 November at 23:53 UT. Only the statistically significant pixels ($\sigma \leq 25\%$) were used for this figure as well as for Figures 3(d) and 8. The contours represent temperatures 7, 9, 10, and 11×10^6 K.

till 22:00 UT even though at least four subflares occurred in AR 17255 in between (*Solar-Geophysical Data*, 1981, 1983; further abbreviation as SGD). At around 21:50 a more important flare (1B–2N, M2 X-ray event) was observed (SGD) and immediately thereafter we could see another revival of the arch as shown in Figures 1(b) and 1(c). The temperature map of the structure is presented in Figure 1(d) and shows T_{\max} high in the corona, like in the earlier arches studied by Švestka. The parent flare was of the two-ribbon type and in $H\alpha$ (see Figure 2) it was almost a copy of the flare that caused

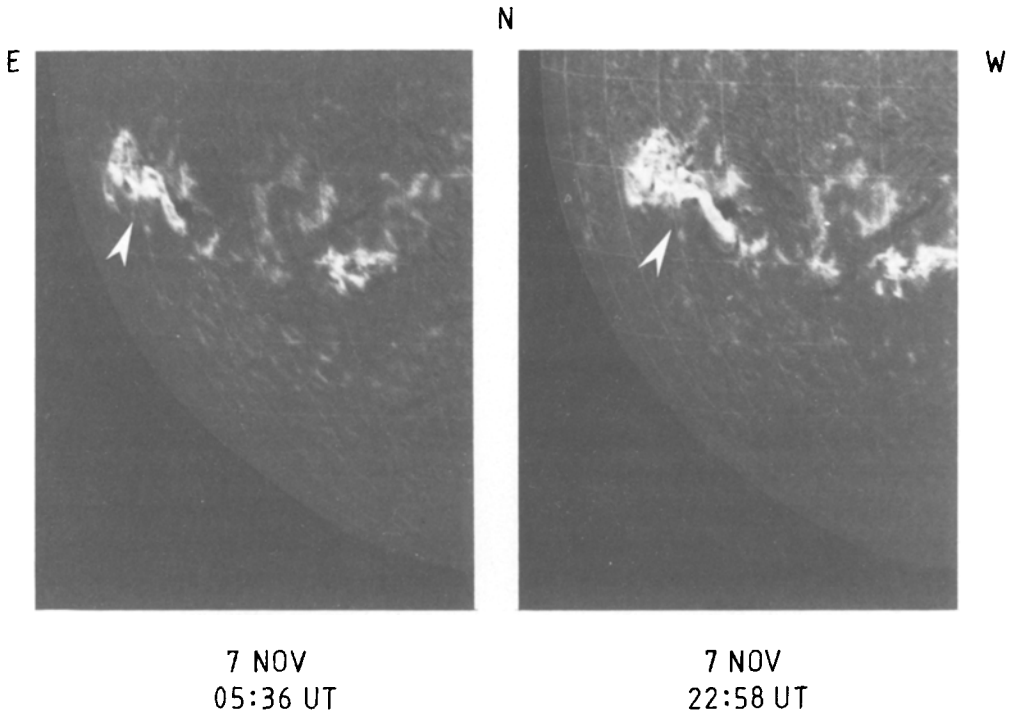


Fig. 2. The parent flares of the last two pronounced revivals of the SE arch. (Courtesy of Culgoora Observatory.)

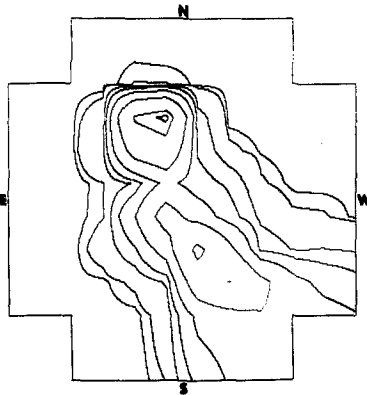
the preceding brightening in the morning hours of the same day. No radio types IV or II were reported in association with these two flares, though this has been a common characteristic of all the other flare-sources of the post-flare coronal arches (Švestka, 1984); both flares, however, were of much smaller importance (1 in $H\alpha$, M in X-rays) than the other events (2 in $H\alpha$, X in X-rays).

Taking into account the homology of the parent flares, similarity in the direction, shape, thermal maps and decay time (≈ 12 h), there is little doubt that the brightening shown in Figure 1 was another revival of the same arch that had been seen and described by Švestka (1984, see Figures 1 and 3 there). Since this family of post-flare arches is being further studied by Hick and Švestka (paper in preparation), we do not analyze these structures here in any more detail.

2.2. NEW CORONAL STRUCTURE EXTENDING TO THE SW

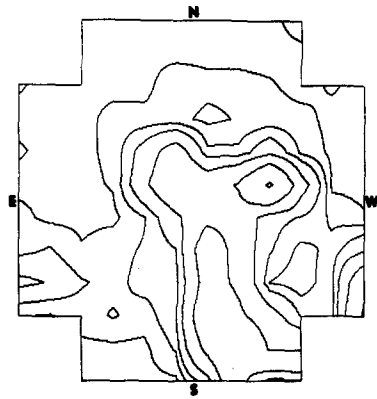
Later on this arch, extending SE, could be seen only once more, very weakly, on 10 November (cf. Figure 3(b)). But on 9 November around 02:30 UT we witnessed the birth of a new arch-like structure extending towards the SW and shown in Figure 3(a). This structure continued to be observable in X-rays also during the following days, with varying intensity. Figure 3(c) shows it, for example, on 11 November and the temperature map of the structure is presented in Figure 3(d).

As Figure 4 shows, there was another region, AR 17251, at a distance of approximately 30° SW from AR 17255. At 01:00 UT on 9 November a rather big flare (1N as



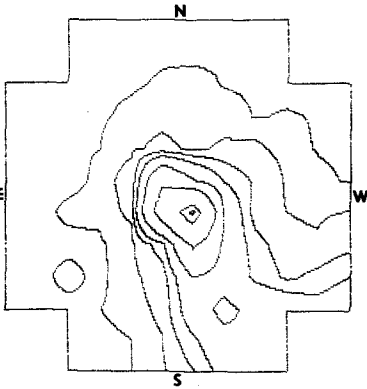
(a) NOV 9, 1980, 04:38 UT

Fig. 3a.



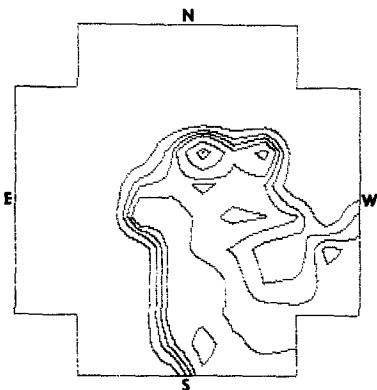
(b) NOV 10, 1980, 14:38 UT

Fig. 3b.



(c) NOV 11, 1980, 06:39 UT

Fig. 3c.



(d) Temperature map

Fig. 3d.

Fig. 3(a-d). Analogous to Figure 1, but (a) 4:32–04:45 UT on 9 November, 1980 (accumulation time 383 s), maximum count rate $7.1 \text{ counts s}^{-1}$ per pixel; (b) 14:25–14:51 UT on 10 November, 1980 (accumulation time 83 s), maximum count rate $0.19 \text{ counts s}^{-1}$ per pixel. Here, the 0.5% level is omitted. (c) 06:32–06:43 UT on 11 November, 1980 (accumulation time 327 s), maximum count rate $19.3 \text{ counts s}^{-1}$ per pixel. (d) The temperature map derived from the 3.5–5.5 and 5.5–8.0 keV energy bands on 11 November at 06:39 UT. The contours represent temperatures 8, 10, 11, 12, 14, and 17×10^6 K.

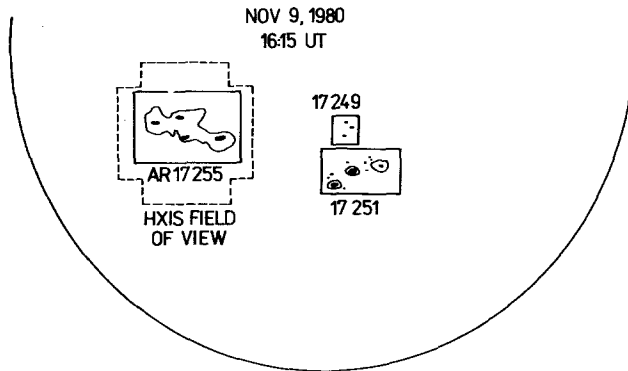


Fig. 4. Photospheric situation on 9 November, 1980.

SGD mean value, three stations out of 8 giving 1B and one station 2B values) appeared in this SW region, probably the largest flare event during its whole existence (cf. Figure 5). Thus, though other flares (the biggest of them 1B – the maximum value of SGD importances) also appeared in the eastern active region, an association with the major flare in AR 17251 seems strongly indicated. The shape and direction of the new structure together with the fact, that it appeared $1^{\text{h}}30^{\text{m}}$ after the major flare in the SW region (the last previous observation without any arch-like structure was done between 01:15 and 01:58 and this defines the uncertainty of the enhancement onset) has lead us to the suggestion that the observed structure was an interconnection of the two active regions visible in X-rays at energies between 3.5 and 8.0 keV.

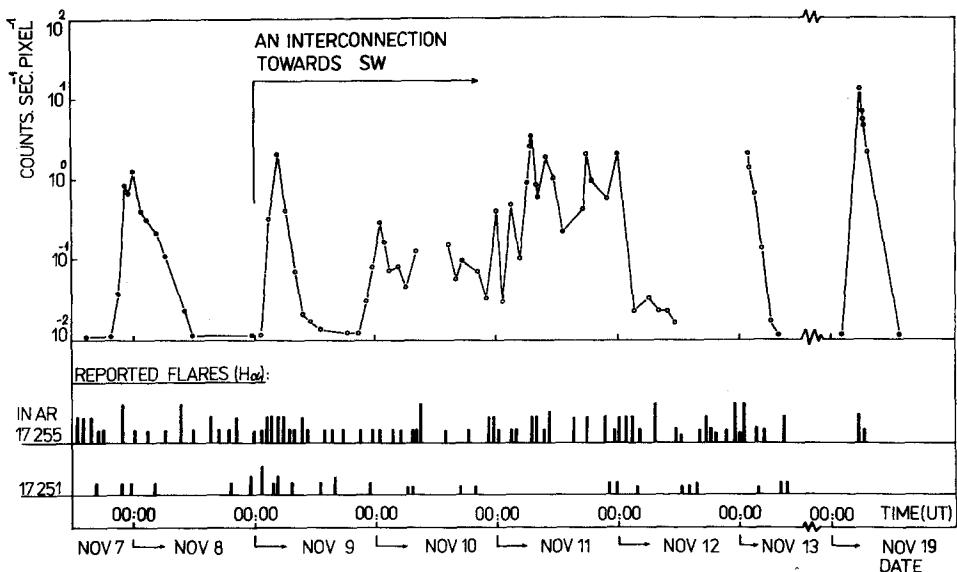
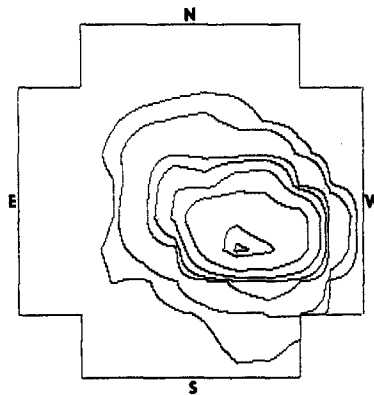


Fig. 5. Time variations of the brightness of the last revival of the SE coronal arch on November 7/8 (dots) and of the interconnection (circles). Reported flares in Hz (SGD; Rust et al., 1982) and their importance are approximately marked.

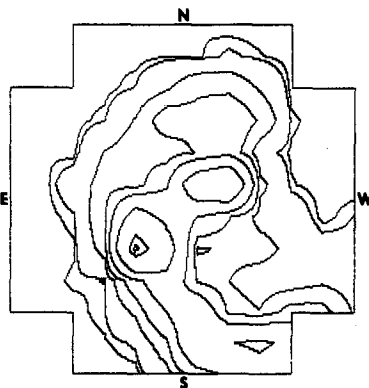
On 10 November between 04:00 and 16:00 UT we observed both the interconnection towards the SW (hereafter we will speak about interconnection to distinguish the new structure from the previous arches) and at the same time a very faint revival of the SE arch (cf. Figure 3(b)). This was the last time we could see the reviving arch. Its intensity was nearly at the sensitivity limit of HXIS and after 16:00 UT it never reappeared.

The X-ray intensity of the interconnection fluctuated as can be seen in Figure 5. The intensity variation of the last revival of the SE arch is plotted there for comparison. In our case the intensity determination is often rather uncertain owing to the fact that we see a large part of the interconnection in projection on the active region, which makes it difficult to separate the emission of the interconnection from that of the active region.



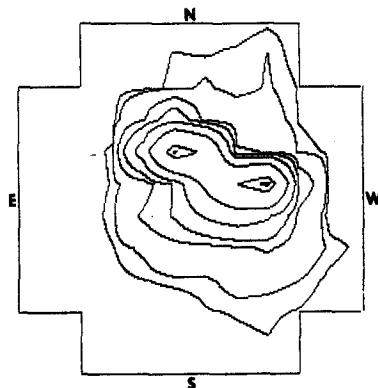
(a) NOV 12, 1980, 08:07 UT

Fig. 6a.



(b) NOV 13, 1980, 03:05 UT

Fig. 6b.



(c) NOV 13, 1980, 07:46 UT

Fig. 6c.

Fig. 6(a-c). Analogous to Figure 1, but (a) 08:01–08:12 UT on 12 November, 1980 (accumulation time 327 s), maximum countrate $11.7 \text{ counts s}^{-1}$ per pixel; (b) 02:55–03:14 UT on 13 November, 1980 (accumulation time 566 s), maximum countrate $1.5 \text{ counts s}^{-1}$ per pixel; (c) 07:33–08:00 UT on 13 November, 1980 (accumulation time 738 s), maximum countrate $1.5 \text{ counts s}^{-1}$ per pixel.

The HXIS field of view is clearly too narrow for a detailed study of such extensive structures.

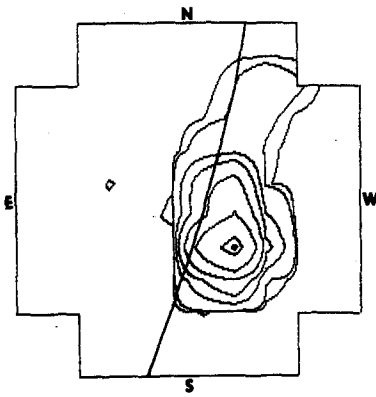
To derive the physical parameters we have read the intensities close to the border of the HXIS coarse field of view in the direction of the interconnection. While the onset phase of the visibility of the interconnecting structure seems to be related with a flare in AR 17251, the later brightenings are most likely associated with flares in AR 17255, if there was any direct flare-association at all. The intensity increased very rapidly after some flares, but it was not influenced by others; for example on 12 November between 07:05 and 07:53 UT a 1B flare was observed in AR 17255 (Culgoora observation, SGD), but in the HXIS data we can not find any other structure than the active region itself during the whole morning (cf. Figure 6(a)). Later on the interconnection revived again, becoming intermittently visible in X-rays as one can see in Figures 6(b) and 6(c). No two-ribbon flare was reported between 8 and 19 November (SGD). Because of technical problems aboard the SMM satellite we have no X-ray data between 13 and 17 November.

On 18 November in the morning we observed a decaying emission of a flare but the possible interconnection was out of field of view. Till midnight no emission other than the remnants of the active region could be observed. On 19 November (when the AR 17255 was close or precisely on the western limb) after a flare in this region had occurred we could observe another revival of the interconnection in side projection (it was during the last day of pointed SMM operations) – see Figures 7(a–d). The interconnecting arch can be separated here from the primary emission of the active region, the maximum of the arch-emission being at height of about 60 000 km above the limb (Figure 7(c)). Figure 8 shows the temperature map of the limb structure.

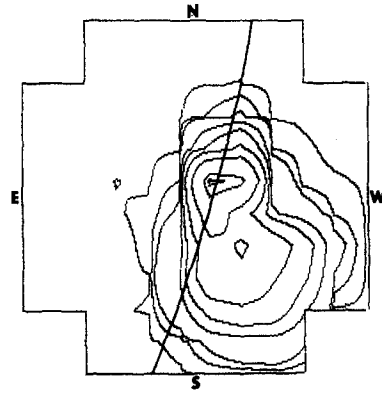
3. Physical Parameters from HXIS Data

We have used count ratio of energy bands 1 and 2 for deriving the temperature. Selected results are presented in Table I. The maximum value of the temperature in the interconnection was found at 06:30 UT on 11 November equal to 14×10^6 K which is the same value as Švestka (1984) found in the SE arch on 6 November. In most other revivals of the interconnection the maximum temperature was somewhat lower, within $8\text{--}12 \times 10^6$ K.

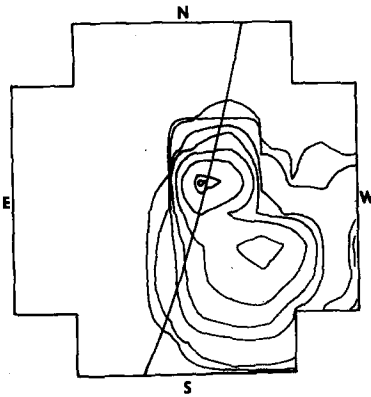
Based on the derived temperature and the measured intensity in band 1 we computed the emission measure. That enabled us to estimate the electron density and the total energy in the interconnection, assuming a tube-like interconnecting loop. Because the active regions were approximately 30° apart from each other we took the length of the interconnecting loop equal to 400 000 km. The diameter of the loop was deduced from the observation on 19 November (side projection of the loop) and was taken equal to 100 000 km because in the unconvolved intensity contour map the loop covers at least four coarse pixels in diameter. To compute the electron density we supposed that the emitting plasma had dimensions corresponding to one coarse pixel in cross-section ($23\,000 \times 23\,000$ km) times 200 000 km in the case of the side projection (on



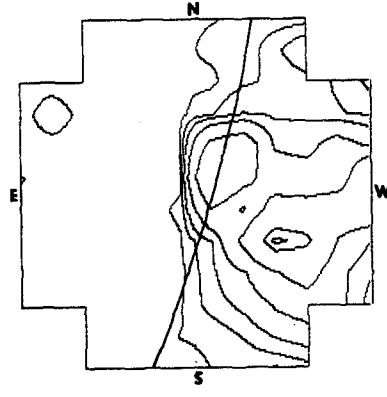
(a) NOV 19, 1980, 02:34 UT
Fig. 7a.



(b) NOV 19, 1980, 05:32 UT
Fig. 7b.



(c) NOV 19, 1980, 06:03 UT
Fig. 7c.



(d) NOV 19, 1980, 07:28 UT
Fig. 7d.

Fig. 7(a-d). Analogous to Figure 1, but for 19 November, 1980. (a) 02:09–02:58 UT (accumulation time 1466 s), maximum countrate 0.84 counts s^{-1} per pixel; (b) 05:30–05:34 UT (accumulation time 120 s), maximum countrate 63 counts s^{-1} per pixel (with an additional contour level 0.1%); (c) 06:00–06:06 UT (accumulation time 189 s), maximum countrate 13.7 counts s^{-1} per pixel; (d) 07:08–07:49 UT (accumulation time 1228 s), maximum countrate 0.22 counts s^{-1} per pixel, with the 0.5% level omitted.

19 November) and, respectively, times 100 000 km when we saw the interconnection on the disc (for example on 11 November). These values are deduced from the assumption on the geometrical form and dimensions of the loop observed by HXIS from the side and from above, respectively. In Figure 5 one can read that the most intense emission was observed during the revival on 19 November at around 05:32 UT. For this time we estimated the total energy of the order of 10^{32} erg ($E = 3kn_eTV$, V being the volume of the interconnecting loop).

Let us estimate the uncertainties of the derived physical parameters.

Let C_1 and C_2 be the count rates in bands 1 and 2 (with the background counts already subtracted). Then their absolute statistical errors are $\sigma_1 = \sqrt{C_1}$, $\sigma_2 = \sqrt{C_2}$, and the

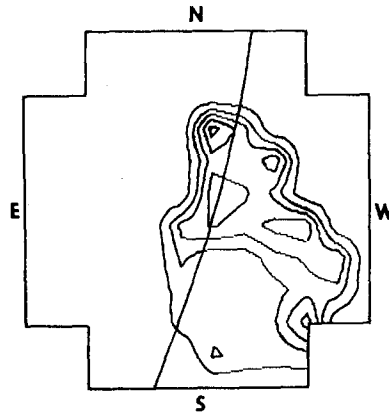


Fig. 8. The temperature map derived from the 3.5–5.5 and 5.5–8.0 keV energy bands on 19 November at around 05:32 UT. The contours represent temperatures 7, 9, 10, 11, and 12×10^6 K.

TABLE I
Physical parameters of the interconnecting loop derived from HXIS data

Date and time (UT)	Position	Temperature (10^6 K)	Maximum countrate	Y (cm^{-3})	n_e (cm^{-3})
9 Nov., 1980 04:39	Pd ^a	10	1.0 ^b	1.0×10^{47}	1.4×10^9
11 Nov., 1980 06:16	Pd	11	0.9	6.2×10^{46}	1.1×10^9
06:30	Pd	14	2.0	6.2×10^{46}	1.1×10^9
07:50	Pd	7.5	0.75	2.5×10^{47}	2.2×10^9
11:22	Pd	8	1.0	2.7×10^{47}	2.3×10^9
19 Nov., 1980 05:32	Pl	10	27.0	2.7×10^{48}	5.0×10^9
06:03	Pl	9	7.2	1.0×10^{48}	3.1×10^9

^a Pd, the most intense pixel in the loop among those close to the edge of the HXIS field of view (to eliminate the contribution of the active region).

Pl, the central (most intense) pixel in the side projection of the loop.

^b Counts s^{-1} per pixel.

error of the ratio $R = C_2/C_1$ is $\sigma_R = R[(\sigma_1/C_1)^2 + (\sigma_2/C_2)^2]^{1/2}$. The interval $(R - \sigma_R, R + \sigma_R)$ corresponds to $(T - \sigma_T, T + \sigma_T)$, σ_T being found in the conversion tables between R and T . The relative statistical error of the ratio R in all the cases is less than 17% and it means the relative error in temperature is less than 6%. The absolute error in T depends upon the used calibration taken from Mewe *et al.* (1986). Taking into account the following relations for emission measure Y and density n_e (thermal emission):

$$Y \sim F\lambda^2 T^{1/2} \exp(144/\lambda T), \quad n_e = (Y/V)^{1/2}$$

(F being the X-ray flux, V the emitting volume, T in 10^6 K) we can derive the uncertainties of Y and n_e , supposing in our case $\lambda \simeq 2 \text{ \AA}$, $T \simeq 10^7$ K and the relative errors of temperature and volume being less than 6% and 50%, respectively. We have found that the relative statistical error of emission measure is less than 50% and that of density less than 70%.

An important information can be derived from the life-time of our structure. While the SE arches observed by Švestka cooled very slowly, the interconnecting arch, whenever enhanced, cooled significantly faster (cf. Figure 5). For example, the arch of 6 November at 14:40 cooled for ≈ 6 hr from $T(0) = 14 \times 10^6$ K to $T(t) = 8 \times 10^6$ K. In the brightened SW structure on 11 November the same temperature decrease was accomplished within 80 min, from 06:30 to 07:50 UT.

For pure radiative cooling, the radiative cooling time from $T(0)$ to $T(t)$ is (Švestka, 1984)

$$t_r = 2.3 \times 10^3 n_e^{-1} [T(0)^{3/2} - T(t)^{3/2}].$$

Thus the n_e value corresponding to $t_r = 6$ hr is $3.2 \times 10^9 \text{ cm}^{-3}$, close to the value of $2.4 \times 10^9 \text{ cm}^{-3}$ found in the SE arch (cf. Švestka, 1984). For $t_r = 80$ m in the SW structure, however, $n_e = 1.5 \times 10^{10} \text{ cm}^{-3}$, apparently too high. Thus either the n_e values in Table I are underestimated – the density in the SW structure being significantly higher than in the SE arch, or an additional cooling by conduction must be taken there into account. This may well be the case in an interconnecting loop. Whereas the post-flare arch must contain a very complex magnetic field (due to successive reconnections) which totally inhibits any conduction along the field lines to lower atmospheric layers, the interconnection is a more simple loop structure so that the magnetic field allows heat conduction into the anchoring footpoints. In any case, the substantially different decay times support the idea that we observed here two different coronal phenomena.

4. Discussion

Our HXIS data resemble pictures of interconnecting loops seen in soft X-rays during the Skylab mission (Švestka et al., 1977; Howard and Švestka, 1977; Švestka and Howard, 1979, 1981), though the physical characteristics of the HXIS structure are strikingly different. In the referred Skylab papers the authors derived the following physical parameters for the loops that interconnect active regions: temperature between 3 and 4 millions K, electron density less than $2 \times 10^9 \text{ cm}^{-3}$ and the most frequent lifetime between 6 and 7 hr. In our case the derived temperature is about 3–4 times higher, density (much more uncertain) somewhat higher, and the mean lifetime of the brightenings is shorter. Reason for these differences is to be found in the different energy ranges of HXIS (3.5–5.5 keV) and the S-054 experiment onboard Skylab (0.23– ≈ 4 keV). Only the brightest (i.e., hottest and most dense) interconnecting loops can be imaged by HXIS, because the brightness of loops with the T and n_e values found by Skylab is below HXIS sensitivity. This is confirmed by the fact that so far only two interconnecting loop systems were tentatively discovered from HXIS data: the one presented here and another one reported on 29 June, 1980 by Harrison et al. (1984).

In the Skylab data many interconnecting loops brightened (Švestka and Howard, 1979), with a rather loose association to flares; it seemed that sometimes the same trigger may produce a flare and enhance a close-by interconnecting loop, but many times only the flare, or only the loop, brightened. A look at Figure 5 reveals that our loop behaved in a similar way. The brightenings on 9 November, AM; 13 November, AM; and 19 November, AM (UT) seem to be associated with big flares in one or the other active region (though chance coincidence cannot be excluded). On the other hand, two flares on 11 November (maximum around 10:10 UT) and on 12 November (maximum around 07:10 UT) did not seem to affect the interconnection at all, and some brightenings (e.g., 11 November in the morning) did not have any obvious flare association with them. Also Harrison et al. (1984), for the interconnecting loop of 29 June, 1980, found flare association with the loop brightenings strongly indicated, but not proved.

We are aware of the fact that our identification of this structure is tentative, because of the small field of view of HXIS. Also the physical parameters can be influenced by the fact that we had to use count-reading close to one of the interconnected regions instead of near to the top of the loop as the Skylab observers could do. Nevertheless, the HXIS data indicate that coronal interconnections between active regions can survive for 10 days or more (as also Howard and Švestka, 1977 found from Skylab data) and that some (though apparently very rare) interconnections can be hotter, denser, and thus contain more energy than the interconnections seen by Skylab. It is perhaps to be noted that the period of HXIS observation was the period of solar maximum, whereas Skylab operated four years after the maximum in the declining phase of the solar cycle. More powerful coronal structures thus could develop in 1980.

5. Conclusions

(1) From 9 November through 19 November (with a gap in data between 13 and 17 November) HXIS possibly imaged in 3.5–8.0 keV X-rays a coronal loop interconnecting two active regions almost 30° apart.

(2) X-ray intensity of this interconnecting loop was greatly variable and its intensity might have been related to flaring activity in the active regions.

(3) If so, then only some flares in the active regions cause revivals of the interconnection. In contradistinction to the post-flare coronal arches, there is no evidence that these need to be two-ribbon flares.

(4) Derived temperature is in the range $7.5\text{--}14 \times 10^6$ K; electron density $n_e = 1.1\text{--}5.0 \times 10^9 \text{ cm}^{-3}$. These values are higher than the values derived from Skylab data in 1973; this fact could be expected because HXIS was measuring in harder energy range and during solar maximum.

(5) The cooling of this interconnecting loop was much faster than the cooling of post-flare coronal arches which indicates that also heat conduction is involved in the cooling process. This suggests a more simple magnetic field configuration in this structure than in the post-flare arches which cool purely by radiation.

Acknowledgements

The authors would like to thank Dr R. E. Loughhead and Mrs W. J. Place of the Culgoora Solar Observatory for providing H α photographs. One of the authors (F. Fárník) was a visiting scientist at the Laboratory for Space Research in Utrecht during this work and thanks SRU staff, in particular Paul Hick, Hans Schrijver, and Chiel Galama for valuable help. The development and construction of HXIS was made possible by support from the Netherlands Ministry for Education and Science, and the Science and Engineering Research Council of the United Kingdom.

References

- Harrison, R. A., Simnett, G. M., Hoyng, P., Lafleur, H., and van Beek, H. F.: 1984, in M. A. Shea et al. (eds.), *STIP Symposium on Solar/Interplanetary Intervals, Maynooth*, p. 287.
- Howard, R. and Švestka, Z.: 1977, *Solar Phys.* **54**, 65.
- Mewe, R., Gronenschild, E. H. B. M., and Van den Oord, G. H. J.: 1985, *Astron. Astrophys. Suppl.* **62**, 197.
- Rust, D. M., Nelson, J. J., Pryor, L. H., Frank, Z. A., and Bogges, A. M.: 1982, *Solar Maximum Year Flare List*, ASA-GSFC.
- Solar Geophysical Data*: 1981, Number 437, Part 1.
- Solar Geophysical Data*: 1983, Number 467, Part 2.
- Švestka, Z.: 1984, *Solar Phys.* **94**, 171.
- Švestka, Z. and Howard, R.: 1979, *Solar Phys.* **63**, 297.
- Švestka, Z. and Howard, R.: 1981, *Solar Phys.* **71**, 349.
- Švestka, Z., Krieger, A. S., Chase, R. C., and Howard, R.: 1977, *Solar Phys.* **52**, 69.